RESEARCH REPORT

VTT-R-07099-10

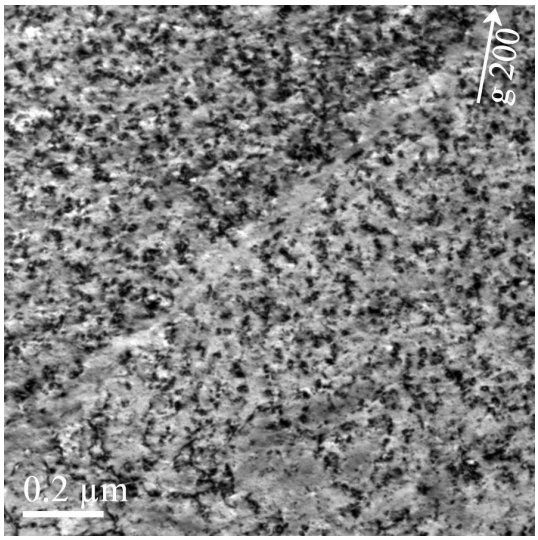

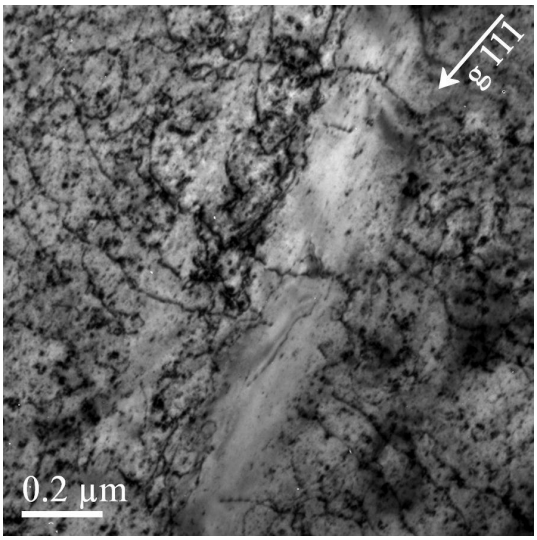

Deformation microstructures of in-reactor tested copper studied by TEM

Authors: Janne Pakarinen

Confidentiality: Public

Report's title	
Deformation microstructures of in-reactor tested copper studied by TEM	
Customer, contact person, address European Fusion Development Agreement EFDA CSU	Order reference TW5-TVV-SITU2
Project name FU-MAT 10	Project number/Short name 70870
Author(s) Janne Pakarinen	Pages 21/
Keywords TEM, in-reactor testing, deformation	Report identification code VTT-R-07099-10

Summary

In-reactor tensile tests of copper have awakened technological and scientific interest due to the reported differences on the tensile behaviour, as compared to tests conducted in the post-irradiated or unirradiated condition. Most distinctly, the rate of post-yield hardening has been shown to increase in the in-reactor tests. Furthermore, the tensile properties drastically change upon irradiation; yield strength of 30 MPa and uniform elongation of 50 % are usually observed for unirradiated copper at 100 °C, while the values for irradiated copper are > 100 MPa and < 15 %, respectively, depending on the irradiation dose.

Post-irradiation tensile tests of copper have shown that plastic deformation occurs in both homogenous and localized fashions. Deformation is generally localized in defect-free channels at irradiation doses higher than 0.1 dpa, although a sparse distribution of such channels have also been observed already at lower doses. Irradiation-induced small defects pin the dislocations and are believed to be the reason for the increased yield strength. While microstructures of post-irradiation deformation experiments are well studied, the deformation microstructures following in-reactor testing are less widely reported.

In this work, microstructures of in-reactor tested copper samples were studied by transmission electron microscopy. One of the samples was subjected to tensile loading immediately upon exposure to neutron irradiation, while other samples were first irradiated for 1 144 and 5 822 minutes before loading was begun. The microstructures showed a sparse distribution of defect free channels and small density of dislocations, while dominating features were dislocation loops and loop-like features. Clear differences in the microstructures between the samples were not detected, but the sample with the highest pre-irradiation showed the highest dislocation density.

Confidentiality	Public

Espoo 17.12.2010

Written by	Reviewed by	Accepted by
Janne Pakarinen, Research Scientist	Seppo Tähtinen Senior Research Scientist	Pentti Kauppinen Technology Manager

VTT's contact address
Kemistintie 3, P.O. Box 1000, FI-02044 VTT

Distribution (customer and VTT)

Preface

This report is a part of the work carried out in Associations Euratom-Tekes by VTT Materials for Power Engineering under the Task TW5-TVV-SITU2 *In-situ Investigation of the Mechanical Performance and Life Time of Copper*.

Contents

1 Introduction

The dynamic effects of deformation and simultaneous neutron irradiation are of particular interest for understanding the behaviour of irradiated materials for life-time management of different components of nuclear power plants (NPP). Most tensile tests of NPP materials that probe the effects of irradiation have been done on irradiated materials in the post-irradiated condition. In these early experiments a clear trend has been established of decreasing ductility and increasing strength with increased dose. Depending on the material's physical properties, neutron irradiation induced displacement cascades induce varying populations of small (from 1 to 10 nm) features like dislocation loops, stacking fault tetrahedra (SFT), and voids.[1] These defects interact with the moving dislocations, causing irradiation hardening and promoting strain localization. By using transmission electron microscopy (TEM) and multiscale modelling with dislocation dynamics, the plastic strain upon initial yielding has been shown to localize in defect free channels.[2] These channels, about 50 - 200 nm wide, propagate through grains at regular intervals, and are generally the most easily resolved deformation microstructures of irradiated materials.

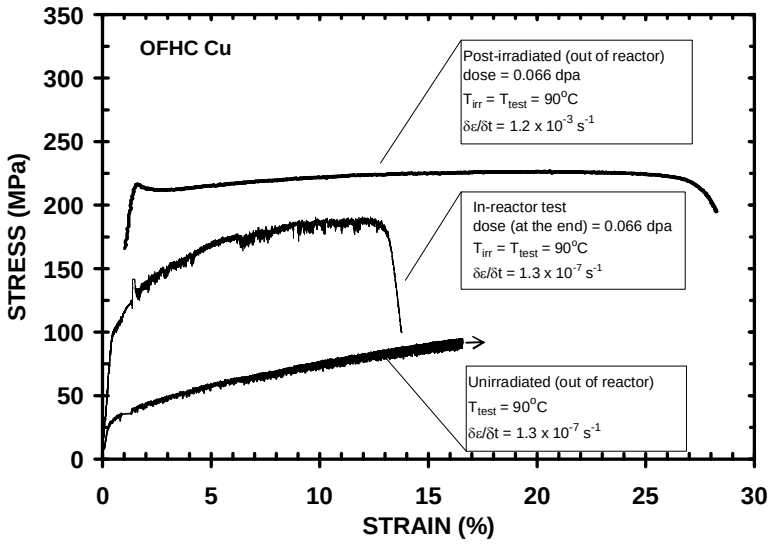

Fig. 1. Comparison of stress-strain curves of in-reactor and post-irradiation tests [3].

Only recently the development of compact and accurately controlled pneumatic in-reactor testing devices has made it possible to study the dynamic response of materials deformed during irradiation. These tensile in-reactor tests have shown that materials properties under simultaneous irradiation and tensile deformation can be different from the stress-strain behaviour of unirradiated samples and of samples tested in the post-irradiation condition. As an example, the tensile in-reactor test result in Fig. 1 (from [3]) shows that the copper sample exhibited significant hardening and a uniform deformation of only about 10 %. In comparison, the tensile tests for unirradiated copper usually show uniform deformation of well over 50 % at the same temperature.[4] The difference between in-reactor and post-irradiation experiments is also well shown in Fig. 1, namely, the post-yield hardening rate of the in-reactor tested sample is much higher than in the case of post-irradiation tests.

A direct comparison between the stress-strain curves of post-irradiation and in-reactor tensile tests is difficult though. In post-irradiation experiments the amount of irradiation defects remains constant, while stress is localized due to dislocation dynamics with further applied stress. With in-reactor tests the population of irradiation defects is constantly evolving. While the microstructures of post-irradiation tested materials are well known and examples have been widely reported, the microstructural response of materials subjected to in-reactor tensile testing is less known. Such characterization is the topic of in this work.

2 Description

The investigated OFHC copper samples were irradiated in the BR-2 reactor at SCK-CEN, according to Table 1. In the tensile tests, the loading of Bar 191 was begun immediately upon start of irradiation, while Bars 193 and 260 were irradiated for 1 144 and 5 822 minutes prior to initiating loading, respectively. The testing was conducted at a slow strain rate of 10^{-7} 1/s, which allows ample time for the simultaneous irradiation to induce microstructural changes. The tensile stress evolution over time for each of the samples is shown in Fig. 2. The testing details can be found from [4]. Notice that the tensile test of Bar 261 was started immediately upon irradiation, but due to computer error the exact test details are unknown.

Table 1. Neutron-irradiation details of the studied samples.

Spec. No.	**Displacement dose (dpa)**				**Damage rate**	**SFT density**[5]
	DST[1]	**DYP**[2]	**DET**[3]	**DEI**[4]		
	[10^{-3}]	**[10^{-3}]**	**[10^{-3}]**	**[10^{-3}]**	**[10^{-8} dpa/s]**	**[10^{23} m^{-3}]**
191	0.02	1.9	9.8	9.8	4.3	3.6
193	3.1	3.1	10.2	10.2	4.5	3.7
260	20.9	23.0	36.7	36.9	6.0	5.2
261	0.02	xxx	xxx	25.1	4.1	4.5

[1]) Dose at the Start of the Test
[2]) Dose at Yield Point
[3]) Dose at the End of Test
[4]) Dose at the End of Irradiation
[5]) SFT density determined in [5]
xxx) Test failed

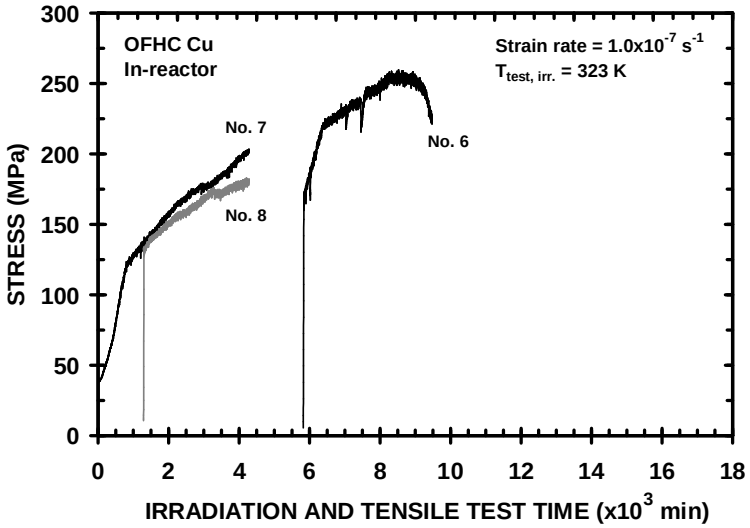

Fig. 2. In-reactor tensile curves for Bars 191(No. 7), 193 (No. 8), and 260 (No. 6).[6]

TEM specimens were punched directly from the 0.3 mm thick test bars. Geometry and dimensions of the bars are shown in Fig. 3 (a). The white circle in (b) shows the approximate position and size of the TEM disc. If the bar was broken, the sample was taken as close to the fracture as possible. After wet grinding the blanks to 0.1 mm, electrolytic polishing by using H_3PO_4 based Struers D2 electrolyte was done with optimized parameters (U ~ 12 V, I ~ 200 mA). After polishing, the samples were quickly transferred to the TEM to minimize the amount of surface oxidation and contamination.

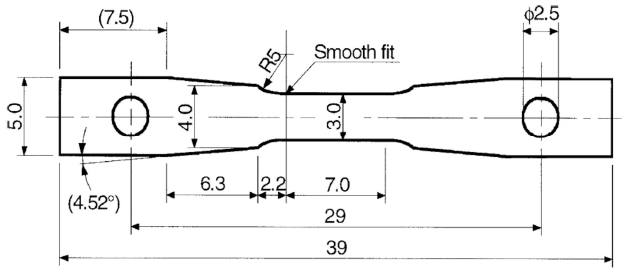

(a)

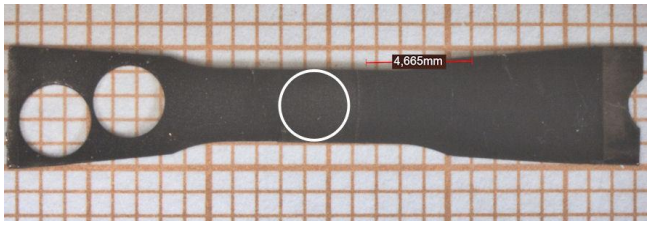

(b)

Fig. 3. (a) Geometry and dimensions of the tensile test bars. (b) Studied test Bar 261. White circle shows the punched TEM specimen size and position. The head sections (visible holes on the left side) were used for irradiation damage analysis. Notice that the undeformed heads were cut off before the samples were shipped

from SCK-CEN to VTT.

3 Results

A large number of images (altogether over 1000) were taken from this series of samples. In addition to the microstructures of the central regions, the less deformed head sections of Bar 191 were used for the characterization of the less deformed and irradiated microstructure. Also, the heads of all the samples were used for SFT density determination (reported in [5]).

The TEM results are presented in the form of image sets. Each image set consists of six images per sample. Central parts of all four of the bars were examined and altogether five samples were fabricated from the head sections of Bar 191. The image sets with captions are given below.

3.1 Bar 191

The tensile test of Bar 191 was started almost immediately, e.g., within 5 minutes, after the rig was inserted to the reactor core. The tensile test was interrupted after 2.3% total strain which corresponds to about 2% plastic strain. The displacement doses at the yield point and at the end of the tensile test were 1.9 and 9.8 x 10^{-3} dpa, respectively (Table 1).

Figs 4-6 shows the microstructure observed in the gauge length region of Bar 191. The microstructure is characterized by a homogeneous distribution of loop-like features and well developed dislocation loops. In addition to these features only few dislocation segments and a sparse distribution of cleared channels was observed. The microstructural features are labelled to Fig. 4 (a). Notice, that the change of the imaging condition from **g** = (200) (Fig. 4 and 5) to **g** = (111) (Fig. 6) did not make any major difference on the observed microstructure. The observation further confirms that the dislocation density was low for Bar 191.

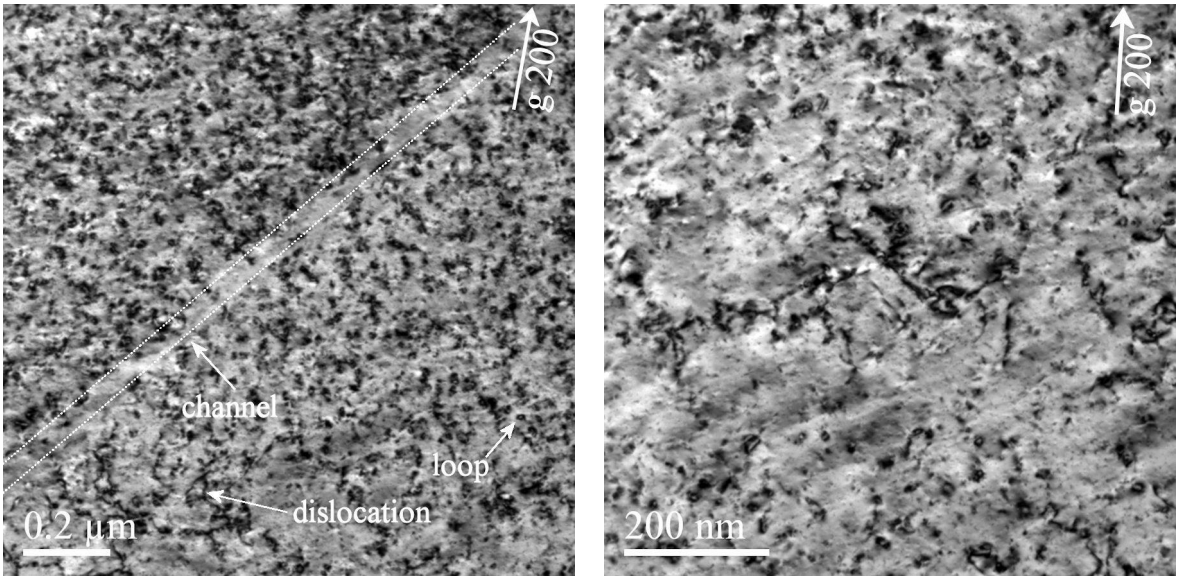

(a) *(b)*

*Fig. 4. Microstructures of Bar191 [**g** = (200)]. The main features of microstructure are labeled to the low magnification image (a); cleared channels, dislocations and dislocation loops. In addition to the well resolved loops some features resembled segments of dislocations or faulted loops (hereafter these features all called loop-like features). A magnified view is given in (b). Even though a few dislocations were detected, loops and loop-like features were the dominant features observed in this sample.*

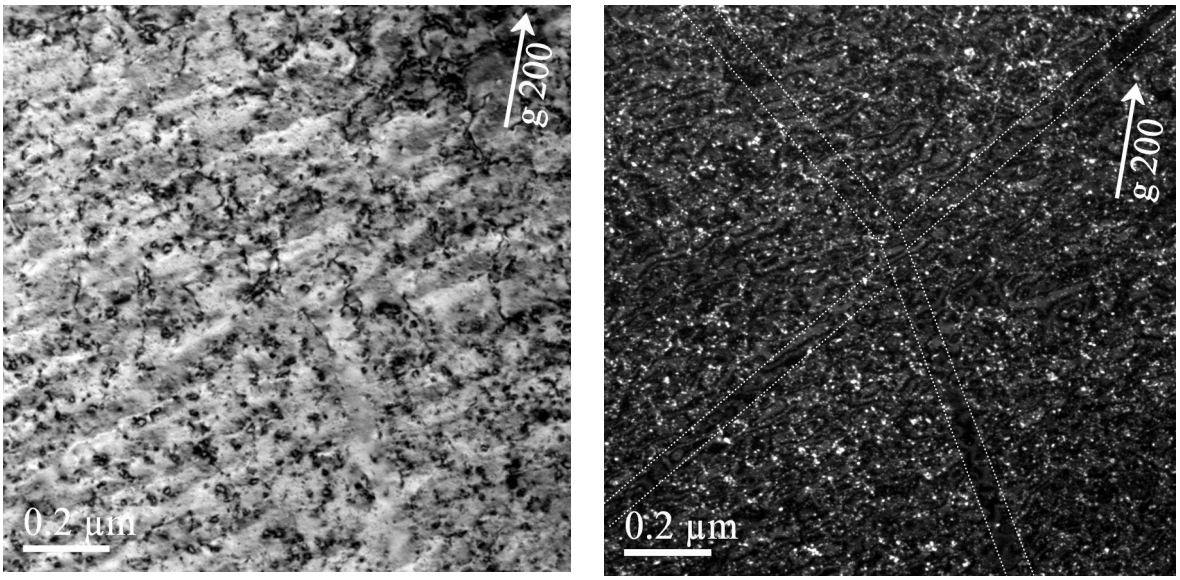

(a) *(b)*

*Fig. 5. Sometimes the cleared channels were difficult to observe in Bar 191 in normal bright-field conditions. Changing the imaging conditions from dynamical 2-beam (a) to (**g**,3**g**) weak beam dark field (b) resolved the channels more clearly.*

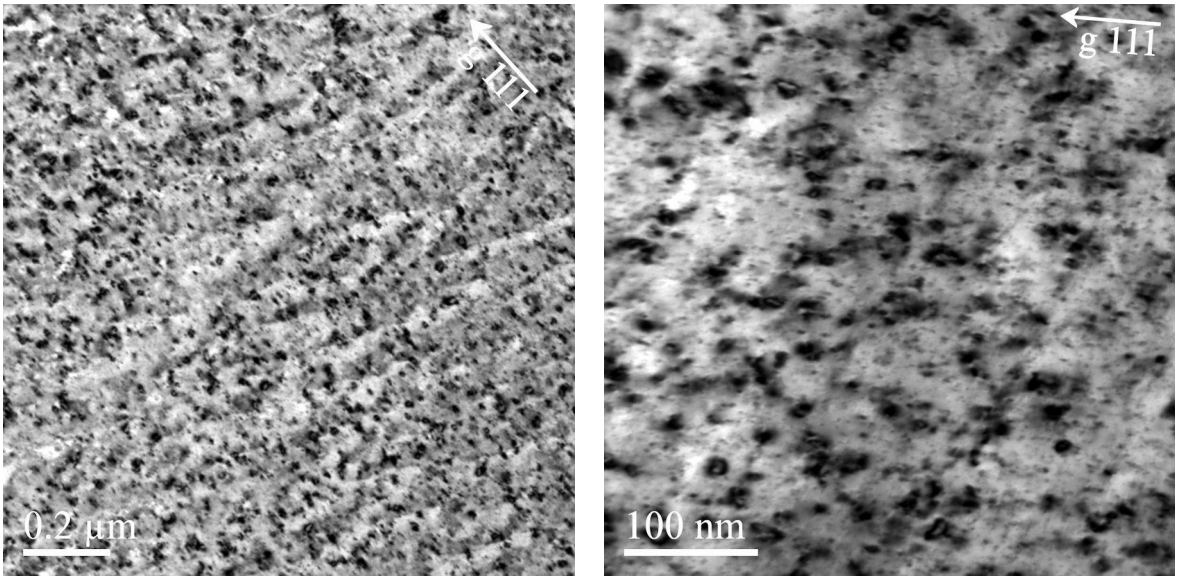

(a) (b)

*Fig. 6. Microstructures of Bar 191 by using **g** = (111) with smaller (a) and larger (b) magnification. The overall microstructure is characterized by loops and loop-like features as previously.*

3.2 Less deformed region of Bar 191

The microstructure of the less deformed region of the bar 191 was similar to that observed in the central gauge length region. Figures 7-9 show that loop- like features and dislocation loops dominate the microstructure and only few cleared channels and dislocation segments can be observed. Again, not much difference was seen in the microstructure when **g** was changed from (111) to (200) [Fig. 7 (a) and (b)].

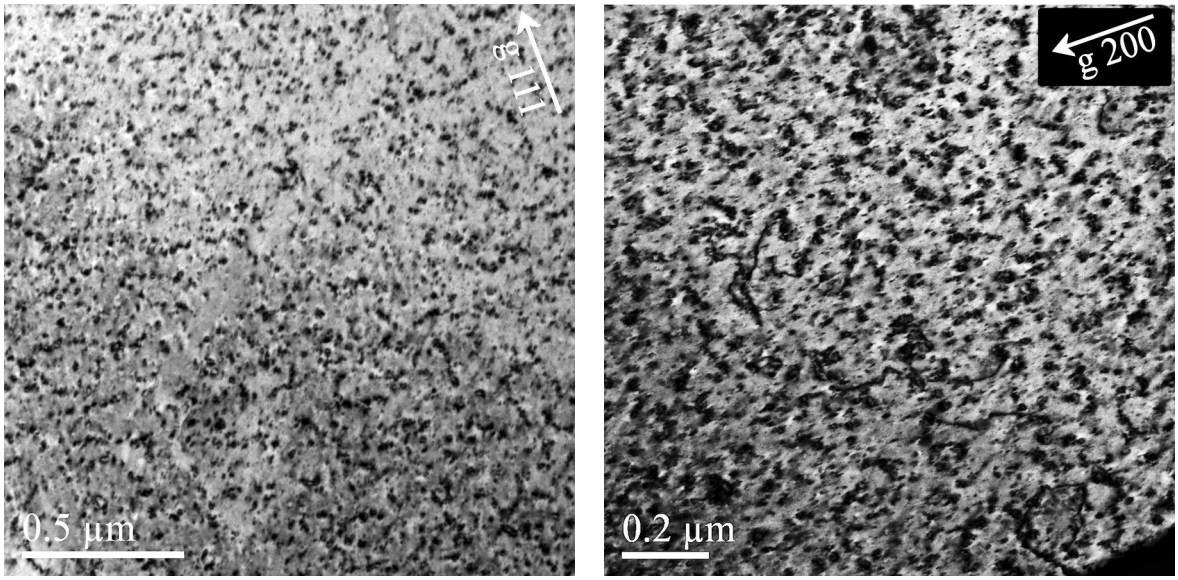

(a) *(b)*

Fig. 7. (a) Low magnification image from the head section of Bar 191 showed that the microstructure was characterized by channels, loops and loop-like features. Higher magnification in (b) shows some dislocations but loops and loop-like features dominate the scene.

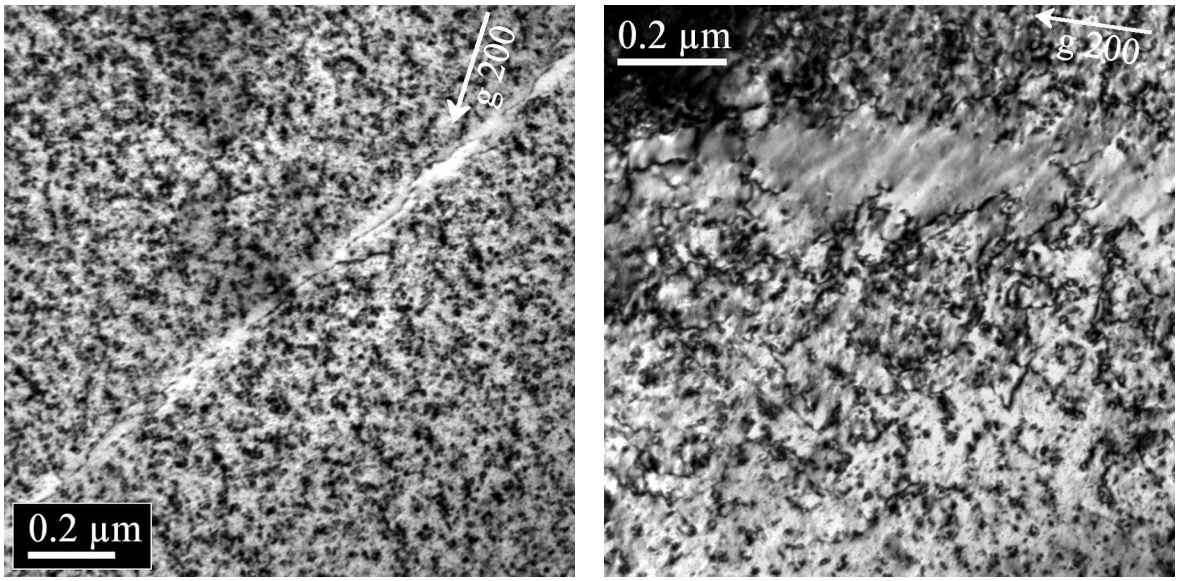

(a) *(b)*

Fig. 8. (a) Even though the head of Bar 191 was less deformed, cleared channels were observable. (b) Some traces of dislocations were also observed. Not much difference was found when comparing the head section to the central part of Bar 191 (Figs 4 -6).

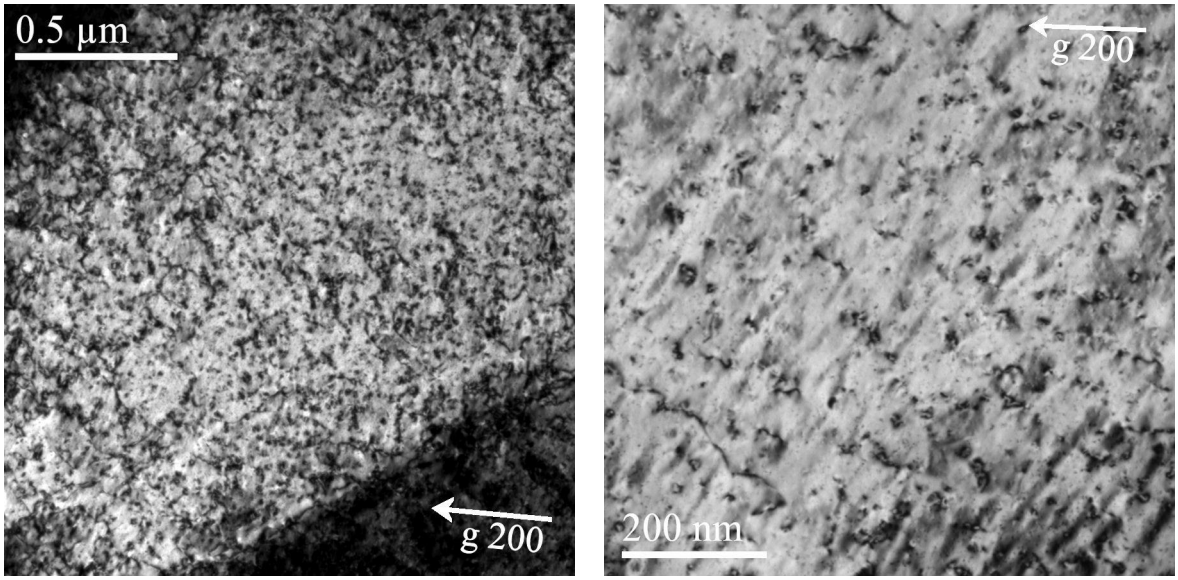

(a) *(b)*

*Fig. 9. (a) Irradiation damage imaged by using **g** = (200) and low magnification. The appearance was quite similar to the samples examined previously. The high magnification image from a thin part of the sample in (b) with **g** = (200) shows few dislocations, loops, and loop-like features.*

3.3 Bar 193

Bars 191 and 193 were irradiated in the same irradiation rig but the tensile tests were initiated at different times in order to vary the displacement dose level before and during the tensile test. The tensile test of Bar 193 was initiated after 1442 minutes of irradiation (Bar 191 had a pre-irradiation of about 5 minutes) and the test was interrupted after 2.0% total strain which corresponds to about 1.6% plastic strain. The displacement doses at the yield point and at the end of the tensile test were 3.1 and 10.2 x 10^{-3} dpa, respectively (Table 1). The tensile tests for Bar 191 and 193 were interrupted simultaneously and at the same time the irradiation rig was pulled out from the reactor core.

The microstructures of Bar 191 and 193 were very similar. Both were dominated by a homogeneous distribution of loop-like features, well developed dislocation loops, and a sparse distribution of cleared channels. The amount of dislocation segments seemed to be somewhat higher in Bar 193 than in Bar 191.

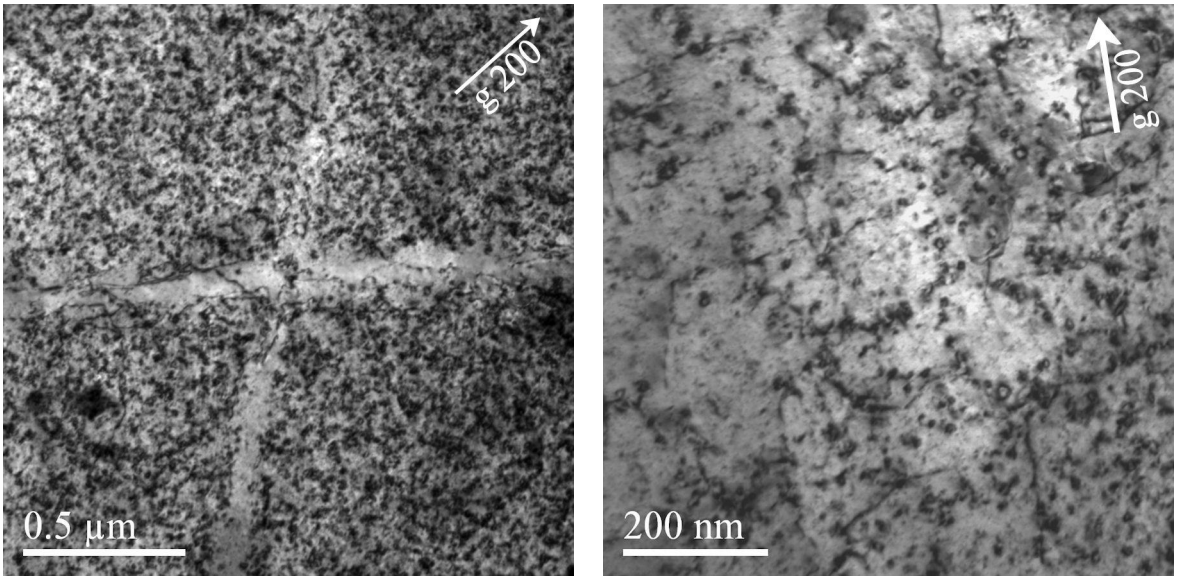

(a) *(b)*

Fig. 10. The stress-strain curves for Bar 191 and 193 were quite similar despite Bar 193 had a pre-irradiation of 1 144 minutes. The microstructures of these bars also have significant similarities; some channels were found (a) and here and there were some dislocations (b). The microstructure was characterized by loops and loop-like features as previously.

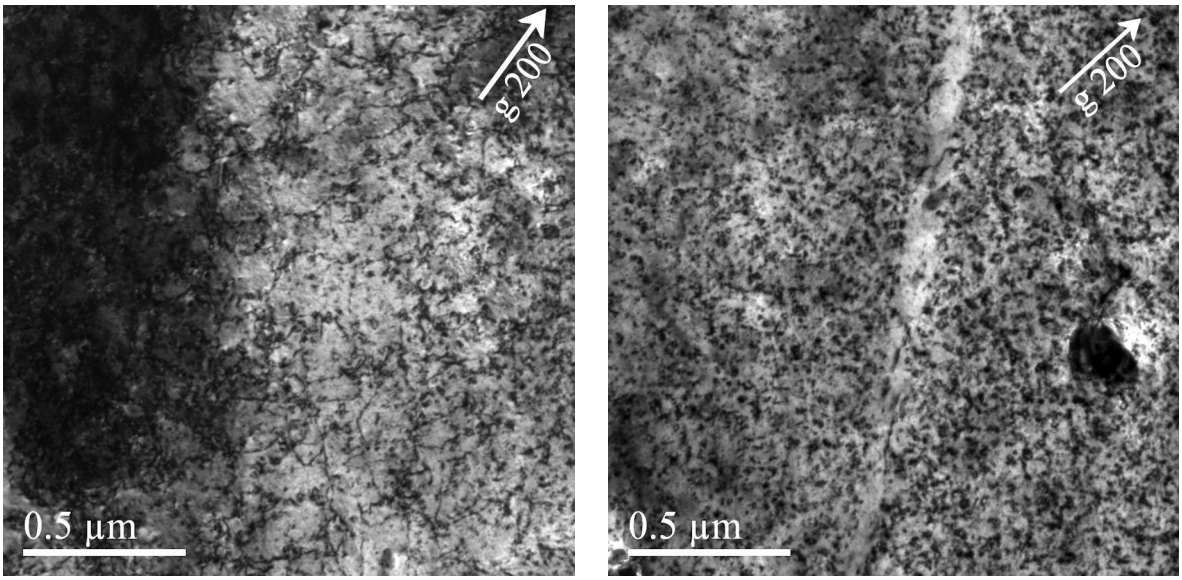

(a) *(b)*

*Fig. 11. Microstructures of Bar 193 by using **g** = (200). Some dislocations are visible in (a), while (b) shows one cleared channel. Loops and loop-like features dominate the view in both images.*

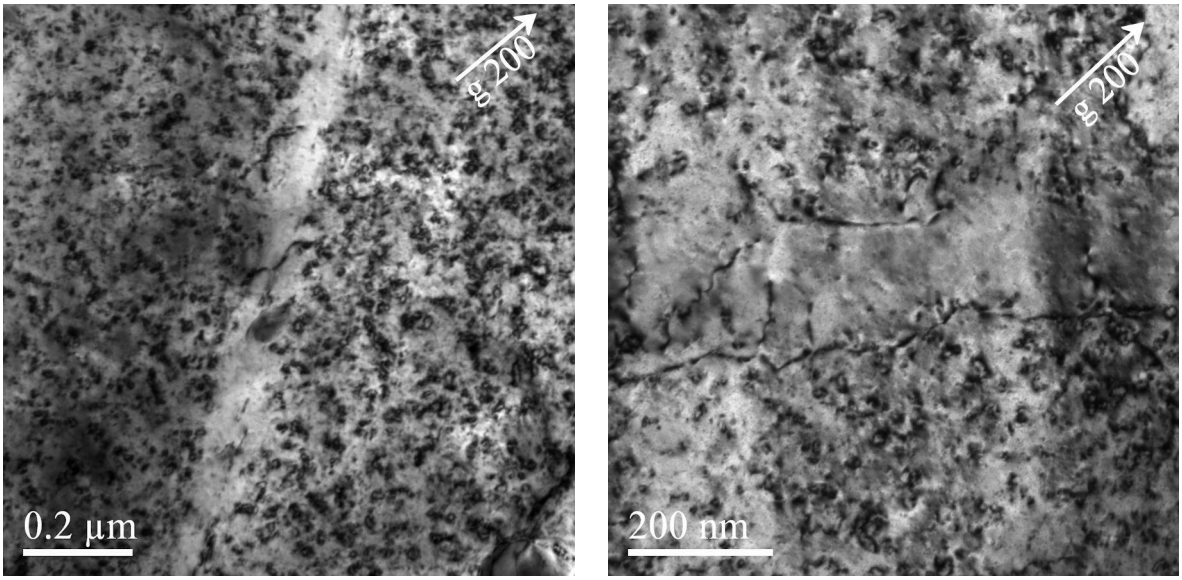

(a) *(b)*

Fig. 12. Some channels from Bar 193. Loops and loop-like features dominated the regions adjacent the channels (a), while some dislocations were detected at the channel (b). Notice, that the dislocations inside the channels are tangled, which most likely is due to irradiation damage (SFT, for example, are too small to be seen at the images).

3.4 Bar 260

Bars 260 and 261 were irradiated in the same irradiation rig. The tensile test of Bar 261 was initiated almost immediately, while Bar 260 was first irradiated 5822 minutes. It was noticed soon after the tensile test of Bar 261 had been started that it was uncontrolled and the loading was interrupted. As a result Bar 261 experienced neutron flux without any external loading most of the testing time.

The tensile test of Bar 260 was interrupted after total strain of 3.7% before complete rupture of the specimen corresponding to about 2% plastic strain. The displacement doses at the yield point and at the end of the tensile test were 23.0 and 36.7 x 10^{-3} dpa, respectively (Table 1).

The microstructure of the in-reactor deformed bar 260 is shown in Figs 10-12. The microstructure of Bar 260 was again dominated by homogeneous distribution of loop-like features and well developed dislocation loops. It is noted that again only few cleared channels were observed. The amount of visible dislocation segments was clearly higher for Bar 260 as compared to Bars 191 and 193.

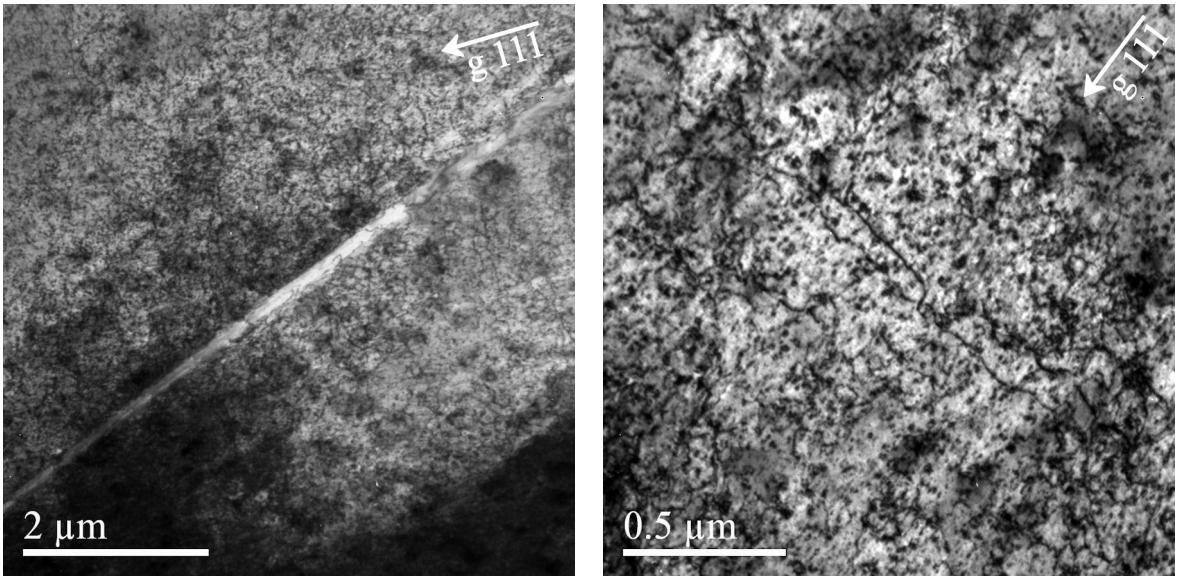

(a) *(b)*

Fig. 13. Low-magnification image of Bar 260 in (a) shows that channels and other irradiation damage were present in this sample, too. While increasing the magnification (b), the existence of dislocation was observed even using ***g*** *= (111), which reveals less dislocations that the* ***g*** *= (200) used in many of the previous pictures. Loops and loop-like features were observed as previously.*

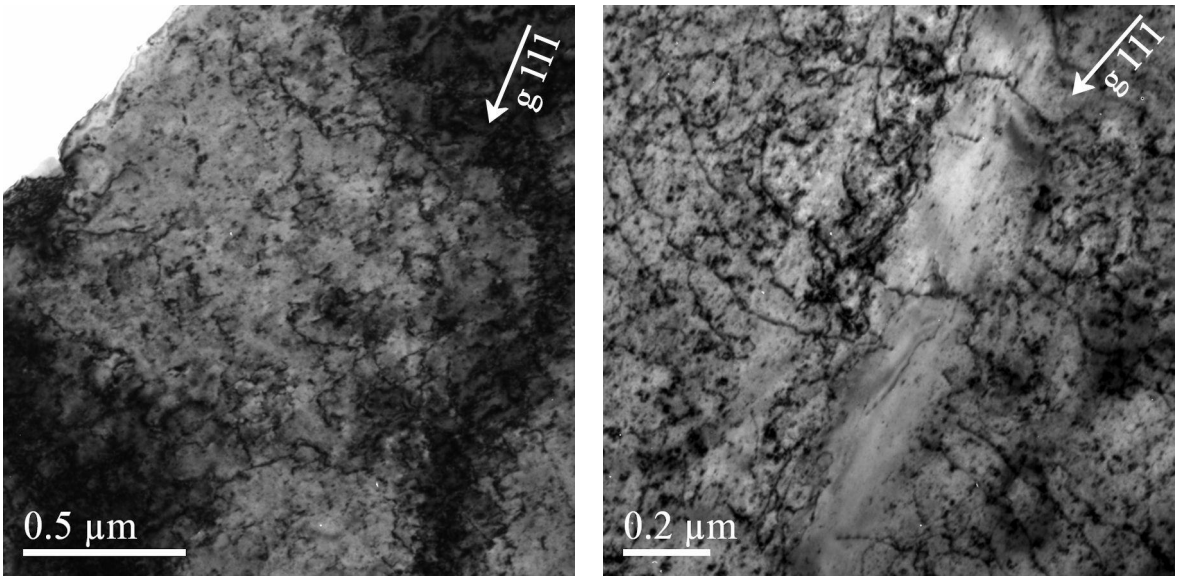

(a) *(b)*

Fig. 14. Dislocations were observed even at the thin regions, as displayed in (a), although the loop-like features were also present in this microstructure. Higher magnification in close proximity of a channel in (b) further confirms the observation of greater dislocation density as compared to Bars 191 and 193 (compare, for example, to Fig. 12 (b), where the samples may be assumed to be about the equal thickness).

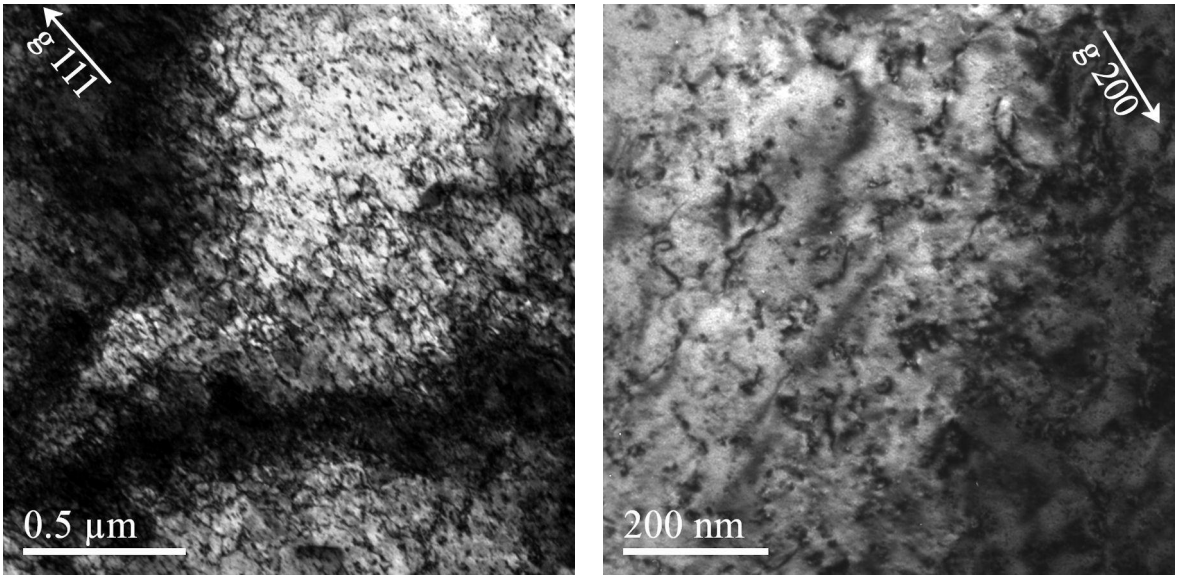

(a) *(b)*

Fig. 15. (a) A general view of Bar 260 microstructure consists of dislocations accompanied by irradiation defects. (b) High magnification view from a thin portion of the Bar 260 reveals the presence of loops and loop-like features.

3.5 Bar 261

The microstructure of the in-reactor deformed Bar 261 is shown in Figs 16-18. It is noted that even thought the tensile test of the bar 261 was started almost immediately, e.g., within 5 min after inserting the specimen in the neutron flux, the tensile test itself was uncontrolled and interrupted soon after it started. This means that Bar 261 experienced plastic deformation in the early state of the irradiation but stayed most of the time without any external stress in the neutron flux. The microstructure of Bar 261 was dominated by a homogeneous distribution of loop-like features and well developed dislocation loops. Very few cleared channels were observed and the dislocations segments were hardly observed.

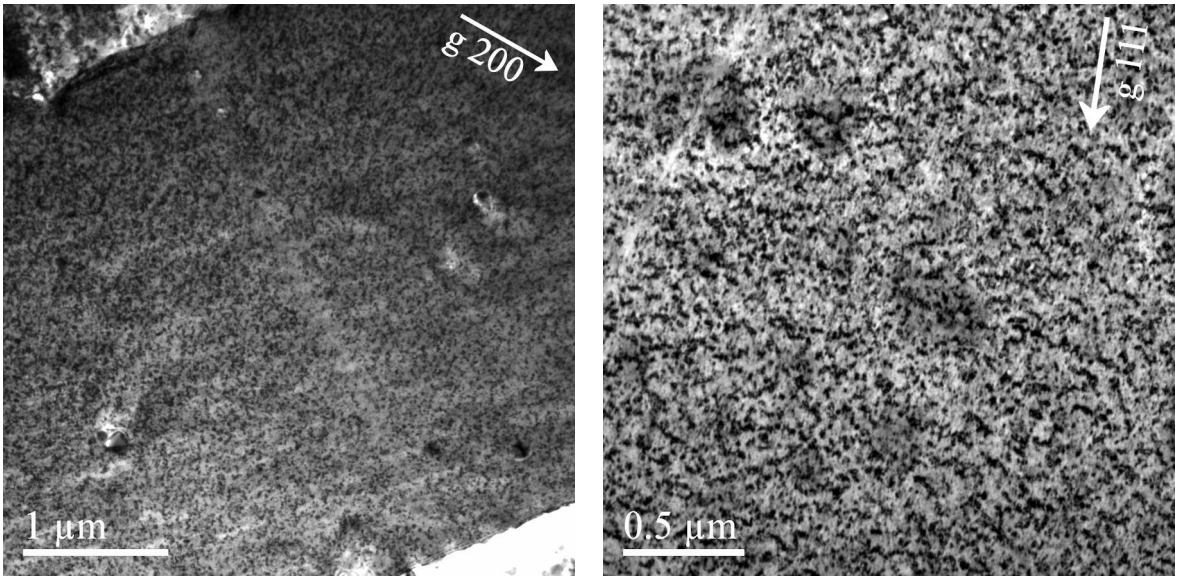

(a) *(b)*

Fig. 16. Low magnification images of Bar 261 showed a pretty similar view to that seen for samples 191 and 193. A sparse distribution of channels (a) and irradiation damage seen in the form of loops and loop-like features (b).

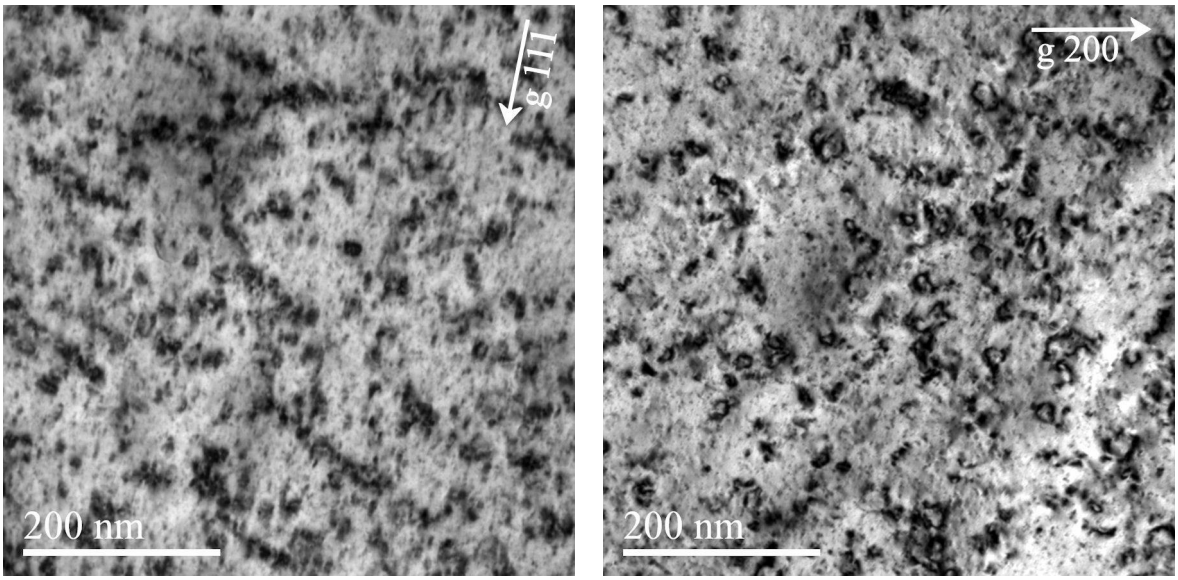

(a) *(b)*

*Fig. 17. High magnification images of Bar 261 showed a small density of dislocations. Loops and loop-like features again seemed to be the dominant feature. Note that changing the diffraction vector from (a) **g** = 111 to (b) **g** = 200 did not bring out dislocations into visible conditions thus suggesting that their density was low for this sample.*

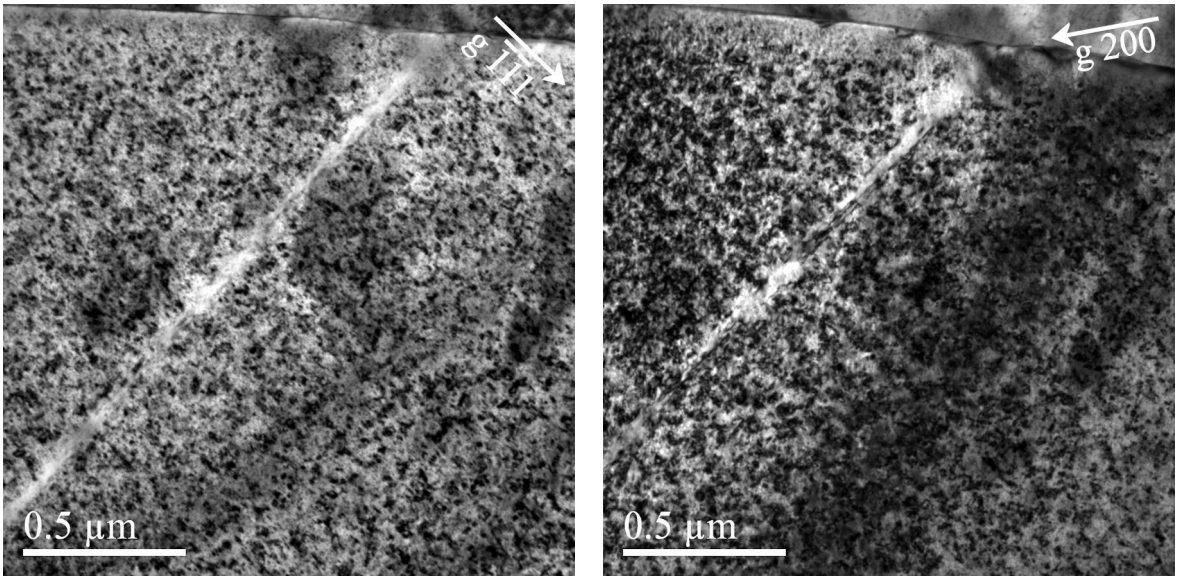

(a) *(b)*

Fig. 18. Thicker region of Bar 261 imaged by using 2 beam conditions with (a) ***g*** *= (-1-11) or (b)* ***g*** *=(200). Again, dislocations were not visible in either of the images, suggesting that they were not present.*

3.6 Summary of the observed microstructures

Table 2 summarizes the observed microstructures and the tensile properties from the in-reactor tests. All the examined samples showed more or less similar microstructure, which consisted of black dislocation loop like features accompanied by a sparse distribution of defect free channels. The observed dislocation density was very small for Bars 191 and 261 (tensile test started nearly immediately). In contrast, some dislocations were found from Bar 191 (pre-irradiation of 1144 minutes) and Bar 261 (pre-irradiation of 5822 minutes), which also showed the highest dislocation density of the studied samples.

In addition to “large” microstructural features, such as dislocations, loop-like features and channels, all the samples had a distinct population of “small” (1-5 nm) SFT. The analysis of these small irradiation defects requires more sophisticated methods in TEM and is reported in [5]. The density of SFT (shown in Table 1) increased upon irradiation dose and was well in line with the values presented in literature.

Table 2. A summary of the tensile properties and microstructural observations for the studied in-reactor samples.

Specimen	Strength [MPa]		Elongation [%]		Microstructure	
	σ_y [1]	σ_{max} [1]	ε_u [2]	ε_t [2]	Feature	Relative amount (> to >>>)
260	218	255	2.8	3.7	dislocations loops[3] channels	>>> >>> >
191	128	212*	2.3*		dislocations loops[3] channels	> >>> >
193	134	185*	2.0*		dislocations loops[3] channels	>> >>> >
261	xxx	xxx	xxx	xxx	dislocations loops[3] channels	> >>> >

[1] $\sigma_{y,\ max}$ = yield strength (y) and maximum (max) strength
[2] $\varepsilon_{u,\ t}$ = uniform (u) and total (t) elongation
[3] including loop-like fetures
xxx) Test failed

4 Discussion and conclusions

Four copper test bars from in-reactor tensile tests were examined by using TEM. The main interest was to characterize the microstructure and determine any differences that may have been evident as a consequence of the different testing and irradiation conditions. The loading of bar 191 was begun immediately after the test module was inserted into the test reactor core, while Bars 193 and 260, respectively, were first irradiated 1144 and 5822 minutes (producing doses of 3.1 $\times 10^{-3}$ and 20.9 $\times 10^{-3}$ dpa) prior to starting the loading. The control of the immediately started tensile test of Bar 261 failed during the test, but the sample was examined anyway.

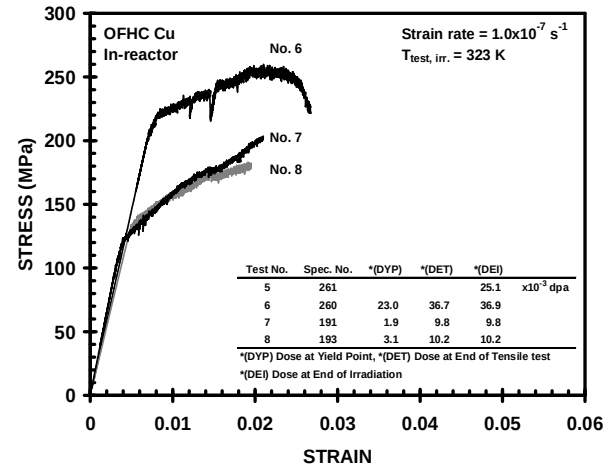

(a)

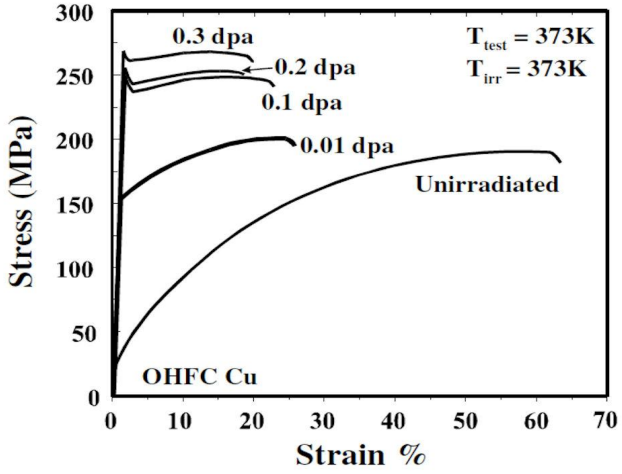

(b)

Fig. 19. Stress-strain curves for (a) in-reactor tested copper [6] *and (b) post-irradiation tested copper* [7].

Comparing the in-reactor stress-strain curves of Fig. 19 (a) to post-irradiation tests of [7] displayed in (b) show major differences in the post-yield hardening behaviour. Namely, the post-yield hardening rate is shown to be much higher in the in-reactor tests than in the post-irradiation tensile tests [notice the nearly tenfold difference between the strain axes of Fig. 19 (a) and (b)]. In both cases, irradiation increases the yield strength of the material as compared to unirradiated reference sample but does not induce any yield drop below dose of 0.1 dpa. The yield strengths are quite nicely in line as a function of irradiation dose [dose at yield point (DYP) values in the case of in-reactor tests], as shown in Fig. 20.

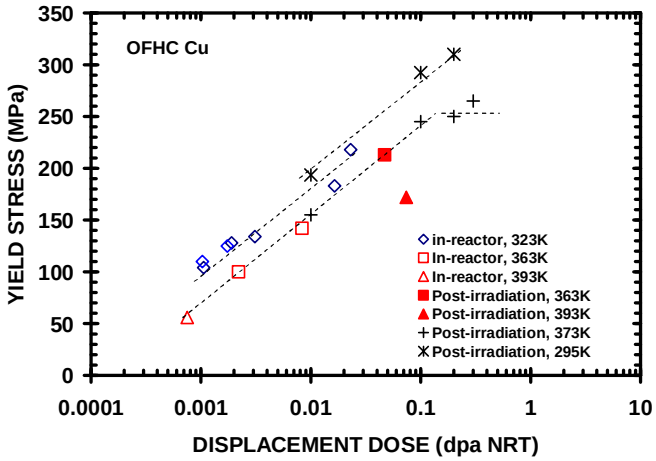

Fig. 20. Yield strengths of in-reactor (open) and post-irradiation (solid) tested copper. The studied samples are from the series labeled with open diamonds. Lines show that the yield stress – displacement dose relationship tends to be dependent of temperature. (◊ from [6], □, Δ, ■, *and* ▲ *from* [8], + *from* [9] *and* * *from* [10].

The increase of yield strength upon irradiation (in post-irradiation and in-reactor tests) is linked to the irradiation defects that pin the dislocations thus resisting their movement and hardening the material. Upon increasing the stress level above yield point, the pinned dislocations have enough energy to move and cause plastic deformation. The fact that no difference was seen at the yield strengths between the in-reactor and post-irradiation tests agrees with the explanation. The strong post-yield strain hardening for the in-reactor tested samples is most likely related to dislocation dynamics as well. Whether the effect is solely due to increase of population of irradiation defects or more complex dislocation displacement cascade interactions requires more experimental verification.

The microstructures of all the studied samples showed fairly small density of dislocations. Bar 260 with the highest dose at the yield point, showed the highest dislocation density. The dislocations were arranged quite homogenously and did not show any major segregation. The existence of a sparse distribution of cleared channels in all the samples is in good agreement with previous results in the literature.[9]

To conclude, the stress-strain curves of in-reactor tested copper samples showed remarkable post-yield hardening behaviour as compared to post-irradiation tests. At the same time, irradiation-induced yield stress increased in line with the post-irradiation tests. The highest dislocation density was observed for the sample with the highest pre-irradiation dose, although the observation yet requires more experimental proof. All the studied in-reactor samples had a sparse distribution of defect free channels.

References

[1] M.L. Jenkins and M.A. Kirk, Charachterization of Radiation Damage by Transmission Electron Microscopy, Institure of Physics Publishing, London, 2001.

[2] T.D. de la Rubia, H.M. Zbib, T.A. Khraishi, B.D. Wirth, M. Victoria, and M.J. Caturla, Multiscale modelling of plastic flow localization in irradiated materials, Nature 406 (2000) 871-874.

[3] P. Moilanen and S. Tähtinen, Mechanical testing under simultaneous neutron irradiation, Industrial Systems Review 2005, VTT Industrial Systems. (2005) 90-93.

[4] B.N. Singh, S. Tähtinen, P. Moilanen, P. Jacquet, and J. Dekeyser, In-reactor uniaxial tensile testing of pure copper at a constant strain rate at 90 °C, J. Nucl. Mater. 320 (2003) 299-304.

[5] J. Pakarinen, Quantitative analysis of irradiation defects of in-reactor tested copper by weak beam method in TEM, Espoo, VTT Research Report VTT-R-07064-10, 2010.

[6] S. Tähtinen, B.N. Singh, and P. Moilanen. , Report on in-reactor interrupted tensile tests of OFHC copper - SITU2, Espoo, VTT Research Report VTT-R-07935-08, 2008.

[7] D.J. Edwards, B.N. Singh, and J. Bildesorensen, Initiation and propagation of cleared channels in neutron-irradiated pure copper and a precipitation hardened CuCrZr alloy, J. Nucl. Mater. 342 (2005) 164 - 178.

[8] B.N. Singh, D.J. Edwards, S. Tähtinen, P. Moilanen, P. Jacquet, and J. Dekeyser. , Final Report on In-reactor Tensile Tests of OFHC-Copper and CuCrZr Alloy, Roskilde, Risø Research Report Risø-R-1481(EN), 2004.

[9] B.N. Singh, D.J. Edwards, and P. Toft, Effect of neutron irradiation and post-irradiation annealing on microstructure and mechanical properties of OFHC-copper, J. Nucl. Mater. 299 (2001) 205-218.

[10] B.N. Singh, A. Horsewell, P. Toft, and D. Edwards, Temperature and dose dependencies of microstructure and hardness of neutron irradiated OFHC copper, J. Nucl. Mater. 224 (1995) 131-140.